
This is an electronic reprint of the original article.
This reprint may differ from the original in pagination and typographic detail.

Silva, Pedro E.S.; Lin, Xueyan; Vaara, Maija; Mohan, Mithila; Vapaavuori, Jaana; Terentjev, Eugene M.

Active Textile Fabrics from Weaving Liquid Crystalline Elastomer Filaments

Published in:
Advanced Materials

DOI:
[10.1002/adma.202210689](https://doi.org/10.1002/adma.202210689)

Published: 06/04/2023

Document Version
Publisher's PDF, also known as Version of record

Published under the following license:
CC BY

Please cite the original version:
Silva, P. E. S., Lin, X., Vaara, M., Mohan, M., Vapaavuori, J., & Terentjev, E. M. (2023). Active Textile Fabrics from Weaving Liquid Crystalline Elastomer Filaments. *Advanced Materials*, 35(14), Article 2210689. <https://doi.org/10.1002/adma.202210689>

This material is protected by copyright and other intellectual property rights, and duplication or sale of all or part of any of the repository collections is not permitted, except that material may be duplicated by you for your research use or educational purposes in electronic or print form. You must obtain permission for any other use. Electronic or print copies may not be offered, whether for sale or otherwise to anyone who is not an authorised user.

Active Textile Fabrics from Weaving Liquid Crystalline Elastomer Filaments

Pedro E. S. Silva, Xueyan Lin, Maija Vaara, Mithila Mohan, Jaana Vapaavuori,* and Eugene M. Terentjev*

Active fabrics, responding autonomously to environmental changes, are the “Holy Grail” of the development of smart textiles. Liquid crystal elastomers (LCEs) promise to be the base materials for large-stroke reversible actuation. The mechanical behavior of LCEs matches almost exactly the human muscle. Yet, it has not been possible to produce filaments from LCEs that will be suitable for standard textile production methods, such as weaving. Based on the recent development of LCE fibers, here, the crafting of active fabrics incorporating LCE yarn, woven on a standard loom, giving control over the weave density and structure, is presented. Two types of LCE yarns (soft and stiff) and their incorporation into several weaving patterns are tested, and the “champions” identified: the twill pattern with stiffer LCE yarn that shows the greatest blocking force of $1\text{--}2\text{ N cm}^{-1}$, and the weft rib pattern with over 10% reversible actuation strain on repeated heating cycles. Reversible 3D shape changes of active fabric utilize the circular weaving patterns that lead to cone shapes upon heating. The seamless combination of active LCE yarns into the rich portfolio of existing passive yarns can be transformative in creating new stimuli-responsive actuating textiles.

is relying on one of their two key properties: the link between the state of internal orientational order and the macroscopic shape of the soft elastomer (the other key property being the “soft elasticity”). The equilibrium (fully reversible) elongation and contraction along the local axis of the nematic director, resulting from the change in the underlying nematic order parameter, can be induced by heating to the isotropic phase and then cooling back. There are many other ways of stimulating LCE actuation,^[1] most notably by light, either causing local heating or molecular isomerization of, for example, azobenzene. However, in all cases, in order to have a fast response (and ideally, lower hysteresis), whether it is the heat transfer or light penetration, the sample has to be very thin: either in the form of a thin film or a fiber. Much of today’s excitement in the use of LCE in soft robotics relies on such films, or 3D-printed filament structures.^[5,6]


1. Introduction

After the pioneering work of Finkelmann and Warner in the late 1980s, liquid crystalline elastomers (LCEs) have been considered a promising “smart” material, with rapid developments in the first 20 years.^[1] The potential for LCE applications as artificial muscles, in many areas of technology and medicine,^[2–4]

The earliest example of LCE fibers was attempted by Naciri et al., who simply used a pair of tweezers to pull out fiber from a side-chain LCE melt and demonstrated its alignment and thermal actuation.^[7] Later, a much longer LCE fiber was produced through melt extrusion, demonstrating high alignment and actuation of up to 500%.^[8] The field since then remained relatively static, partially due to the weak mechanical strength of LCE fibers at the time, and partially due to the difficulties in LCEs fabrication. The issues were resolved when thiol-ene click chemistry was introduced into the LCE field in 2015, allowing robust production of larger quantities of main-chain LCEs.^[9] This new chemistry has also revived the interest in LCE fiber fabrication.^[2,10–19] In two particular developments, Roach et al. reported combining LCE fibers with cotton, by simply stitching the LCE onto the fabric, showing that on heating the contracting LCE fibers were producing some shape morphing.^[12] Geng et al. produced ribbon-like yarns of cholesteric LCE with full visible spectrum mechanochromic response and further integrated the filaments into textiles by using the embroidery technique.^[13] In both cases, the “weaving” was achieved by manually placing the filaments into a square pattern, so the resulting low-density meshes were not strictly “textiles”. LCE filaments have never been used directly as yarns in fabrics via conventional textile crafting techniques such as weaving, knitting, lace-making, and crocheting. Here, we report the investigation of some of these

P. E. S. Silva, M. Vaara, M. Mohan, J. Vapaavuori
Department of Chemistry and Materials Science
School of Chemical Engineering
Aalto University
Kemistintie 1, Espoo 02150, Finland
E-mail: jaana.vapaavuori@aalto.fi

X. Lin, E. M. Terentjev
Cavendish Laboratory
University of Cambridge
JJ Thomson Avenue, Cambridge CB3 0HE, UK
E-mail: emt1000@cam.ac.uk

 The ORCID identification number(s) for the author(s) of this article can be found under <https://doi.org/10.1002/adma.202210689>.

© 2023 The Authors. Advanced Materials published by Wiley-VCH GmbH. This is an open access article under the terms of the Creative Commons Attribution License, which permits use, distribution and reproduction in any medium, provided the original work is properly cited.

DOI: 10.1002/adma.202210689

textile crafting techniques, namely weaving and lace-making, in combination with LCE yarns, and the variety of LCE fabrics produced consequently.

The inclusion of sensing and actuation capabilities in smart fabrics can transform the user experience, and potentially give rise to new applications. The improvement of conventional applications by adjusting to individual needs can span from aesthetics, for instance, based on color preferences^[17,21,22] or body shape,^[23,24] to monitoring—for example, recording of physical activities and everyday habits to address health problems.^[25,26] However, simply down-sizing current bulk technologies into textiles is often complicated and compromises user comfort. For example, current e-textiles rely on durable rigid connectors that may negatively impact the form, fit, and function of fabrics.^[27] Therefore, it is highly desirable that the main structural components that compose conventional fabrics are replaced with others that match mechanical features and are long-lasting, without losing the added smart features. Furthermore, implementing new functionality to the yarn-like elements themselves allows the combination of active yarns with traditional textile yarns by employing known industrial processes. In fact, a commercial example of smart actuating fabric made from twisted nylon yarns has been delivered in Winter Olympics 2022 in order to increase the layer thickness (and thus insulation) at cold temperatures.^[28,29] However, this unique example relies on cleverly converting the (small) thermal expansion of plastic into linear actuation along the helical twist axis, based on changing the bending angle, making the amplitude and force delivered quite low.

Incorporating LCE yarn, with fundamentally reversible and large-amplitude actuation, into the mainstream fabric is the concept we explore here. As a result, we showcase the fabrication of 2D and 3D actuating textiles through the seamless integration of conventional textile yarns and active LCE textile yarns. Out of the many possible weaving configurations, we employ several well-recognized patterns and compare their properties. The LCE yarns are found to be compatible with diverse textile fabrication techniques—some of them directly industrial, thus opening a way for the production of novel active fabrics.

2. Results

2.1. Production of Soft and Stiff LCE Yarns

The protocols to produce soft and stiff LCE yarns follow our previous work, and others,^[11,30,31] and are detailed in Supporting Information. This spinning process is easy, scalable, and tunable, since it follows the industry-standard steps, making the scaling-up realistic. Nematic LCE is naturally very sticky.^[32,33] Magnesium stearate powder was used as the anti-sticking agent to coat the yarn surface. Based on optical microscopy, the soft LCE yarns had a uniform diameter of $\approx 170\ \mu\text{m}$, and it did not visibly change when a secondary network was introduced, **Figure 1**. The commercially-available cotton (cellulose) and elastane (polyurethane) yarns used in this work had diameters of $\approx 250\ \mu\text{m}$, however, they are made of multiple filaments twisted together, see **Figure 1b**. The twisting of multiple LCE yarns

was not explored in our current study, but it could be used to further increase the mechanical strength of LCE yarn.^[12] Tensile tests conducted on these four kinds of yarns and the spontaneous load-free elongation on cooling the LCE from the isotropic phase are also illustrated in **Figure 1**. Notably, and expectedly, the actuation amplitude is much reduced by the second network used to mechanically stiffen the filaments.^[20] The filaments could behave very differently: cotton yarn breaks at 5.5 N and close to 15% strain, while elastane breaks at 1.4 N and 850% strain. The single-filament soft LCE yarn had a low elastic modulus before 200% strain but it managed to attain the breaking stress similar to that of stiff LCE yarn. The stiff LCE yarn is more capable than the soft yarns in containing deformation under heavier loads at high temperatures (see Supporting Information).

2.2. Weaving Textiles with LCE Yarn

After producing over 100 m of stable LCE filament, we started by demonstrating that LCE yarns could be directly integrated into textiles. We have selected weaving as the first technique to create textiles with LCE yarn, since it is the most widely used method in the textile industry.^[34] Furthermore, the different weaving patterns are geometrically intuitive as a first case study (see Supporting Information for integration of LCE yarns with the bobbin lace technique). Another distinct advantage of weaving is that contracting/expanding the yarns in a weaving pattern may give rise to a controlled variation of porosity, which is of interest for many futuristic technical textiles, for instance for management of incoming transmitted light, filters, and thermal insulation.

A standard weave consists of an arrangement of perpendicular sets of yarns or ribbons that are interlaced by patterned movements or precise intertwining, forming the fabric.^[35] Generally, the first set of yarns, the warp, is positioned in a loom, evenly distanced, and held under tension. Then, the weft, or filling, is inserted perpendicularly into the warp by either going over and under the warp threads, or the warp threads can be raised and lowered creating a straight open path for the crossing of a shuttle carrying the weft yarn, as illustrated in **Figure 2**.^[35] The cycle of the insertion of a line of weft ends with pushing the yarn line against the already formed cloth: the “beat-up”. The amount of force applied in this step influences the weft density. Different weaving patterns have distinct visual features and impact fabric stability, for instance, the tendency to skew or have seam slippage resulting from the crossovers between warp and weft.^[34]

Weaving structures can be divided into three fundamental categories: plain, satin, and twill weaves. The patterns shown in **Figure 2b** were selected to study the contraction of active yarns depending on the number of floats and crossings along warp and weft. The most elementary pattern is the plain weave, where the maximum interlacing is obtained: each warp yarn alternates over and under the weft yarns, and each weft yarn alternates over and under the warp yarns. The contraction of active yarns will mostly depend on spatial freedom in the weave. For this reason, we also studied how multiple floating influences the fabric actuation using satin, weft rib,

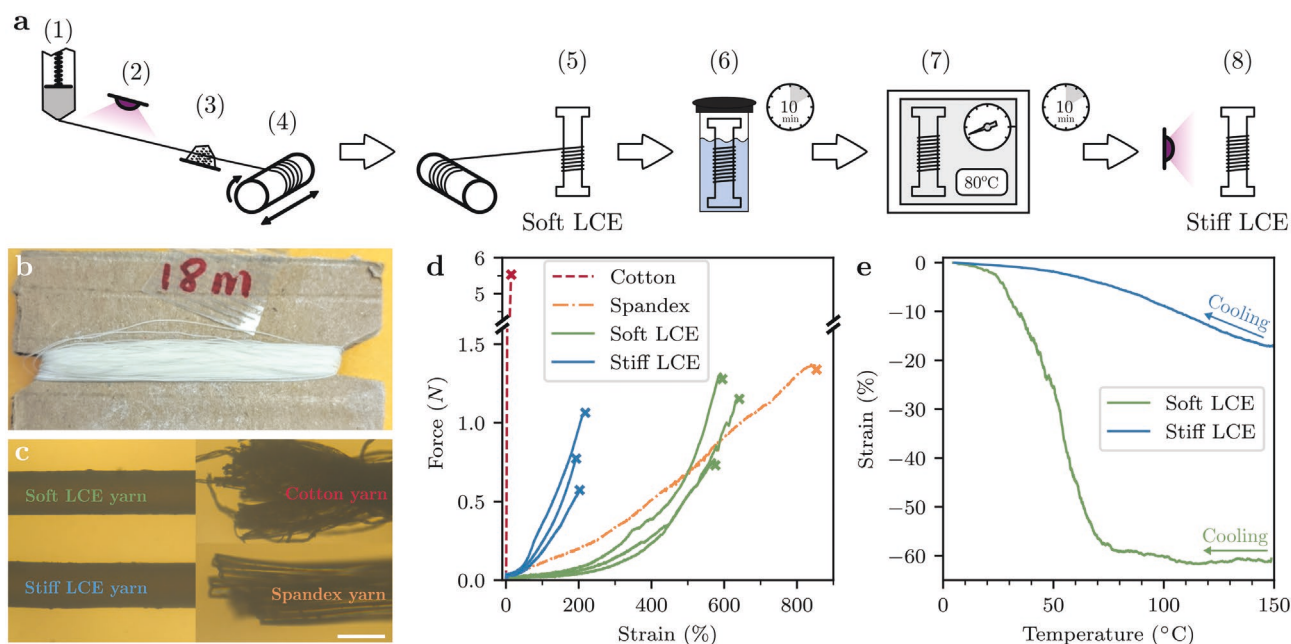


Figure 1. LCE yarn fabrication: a) Consecutive steps of the double-network fabrication process: 1) the viscous filament is extruded and the crosslinking is induced by 2) a 365 nm UV-LED; 3) the filament is passed through a heap of magnesium stearate powder, to make the surface non-sticky, and wound on 4) a rotating collector that moves perpendicularly to the yarn collecting, indicated by the full black arrows. To produce the stiff LCE, 5) the LCE filament is then re-wound on a PTFE dogbone-shaped plate which is 6) immersed in toluene solution with secondary-network monomers to diffuse in, for 10 min; 7) after evaporation of toluene, in an oven at 80 °C, in under vacuum, and for 10 min, 8) the second UV-irradiation forms the secondary network interwoven inside the original thiol-acrylate LCE. b) An illustration of a sample of 18 m stiff LCE yarn wound on cardboard (≈ 400 mg of extrusion content). c) Microscopic images of soft and stiff LCE yarns in comparison with commercial cotton and elastane yarns, scale bar is 200 μm . d) Force–displacement curves of the yarns, of the fixed initial length 25 mm and strain rate 0.1 s^{-1} ; cotton yarn breaks at 15%. e) The cooling actuation curves of soft and stiff LCE yarns, at a cooling rate of 3 °C min^{-1} . As expected, due to their supercritical nature arising from aligned internal constraints, stiff LCE yarns do not reach the actuation plateau at far as 150 °C.^[20]

and twill patterns. Our hypothesis was that weaving designs with a higher number of floating along the warp should have improved contractility, upon actuation of the active weft. The 3/1 satin weave has three warp yarns floating under a weft for every single floating warp over a weft yarn, which makes an unbalanced floating. The 4/4 weft rib, which is a variation of the plain weave and has a similar construction pattern, and 4/4 twill weaves have both alternating four warp yarns floating under and over a weft yarn. Therefore, both 4/4 weft rib and 4/4 twill have balanced floating.

In addition to weaving patterns, the density of a weave can also be preset and controlled during the crafting stage. For denser weaves, the movement of yarns is constricted, which might suppress the actuation of the active yarn. On the other hand, low-density weaves tend to be more unstable, and the prominence of irregularities can lead to random responses when actuating. Therefore, in the first study, fabrics were crafted with tight densities, and most of the actuation would result from the yarn floating. In later experiments, we also examined the effect of yarn density on plain weaves, using stiff LCE yarn, and indeed observed that the lower the density is, the higher the actuation (see Section S3.3, Supporting Information).

The warp used to craft the several fabrics was initially set at a density of 20 yarns cm^{-1} (e.g., 5 cm with 100 yarns), and held under tension. As for controlling the weft density, the loom has a swinging frame, and the beater is used to beat up

the weft yarn onto the weave. The experienced hand-weaver can use approximately the same amount of force by using the weight of the beater. The movement comes naturally and allows the generation of uniform hand-woven fabric samples. However, the same amount of force can generate dissimilar densities depending on the weaving pattern, because of the different numbers of points where the weft crosses between the warp yarns: those points of crossing slow down the beater. For instance, the plain weave with single yarn floats is less dense than the weft rib weave with four yarn floats, Figure 2b. Upon release from the loom, the density of the warp changed roughly to 25 yarns cm^{-1} , Table 1. This contraction, in both directions, is caused by two factors: the warp is set in the loom under tension, and the pulling of the weft during the crossing of the warp threads always generates extension in the weft. The contraction effect is amplified when using elastic threads.

2.3. Actuation of LCE Fabrics upon Heating with Infrared Lamp

After successfully producing a variety of fabrics with soft and stiff LCE yarns, the next step was to test whether the textiles would actuate reversibly upon heating/cooling cycles, and to measure the effect of different weaving structures. We developed an experimental framework to exclude the effects of friction between the textile and a substrate surface, and minimize the bending tendency of load-free fabrics as a consequence of an

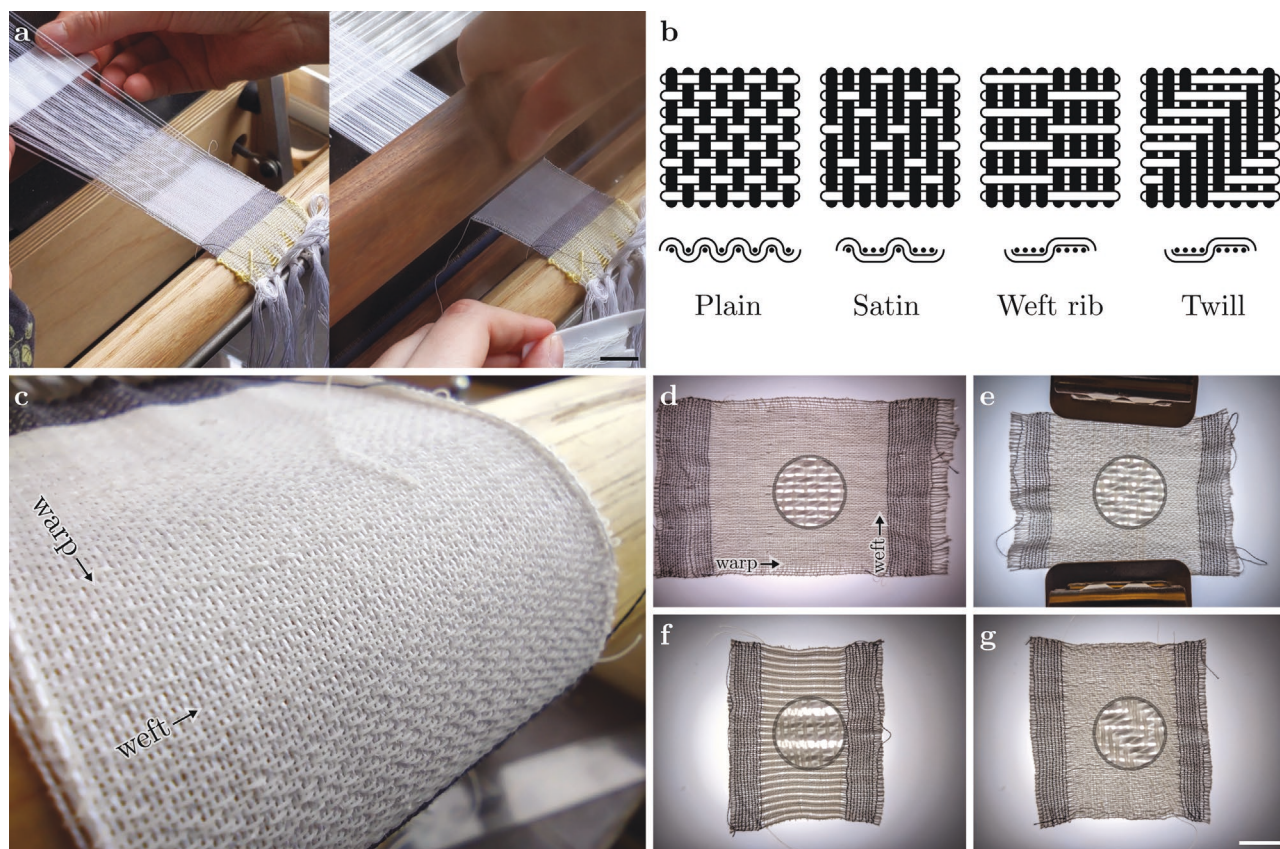


Figure 2. Production of textiles using LCE yarns. a) Sequence of weaving in the loom (see Movie S6, Supporting Information): (left) a shuttle carrying the weft crosses a warp, with yarns that have been raised or lowered, through an open channel; (right) the new line of weft is beat-up into the cloth and, afterward, the computer raises or lowers the heddles to change to a new warp configuration of raised and lowered yarns. Scale bar: 2 cm. b) (top) Four weave diagrams used in this work and (bottom) corresponding floating of the weft, here LCE yarn, along the warp; in all depictions, black and white fill color indicate warp and weft, respectively. c) Cloth with a satin pattern before being removed from the loom. Warp length is 5 cm. d–g) Examples of fabrics after being removed from the loom: d) plain; e) satin; f) weft rib; and g) twill; metal clips were added to the satin weave due to the curling of the fabric along the weft direction. Scale bar in (d–g): 1 cm.

unbalanced floating. The fabrics were suspended and clamped using metallic clips heavy enough to restrict the bending, but light enough not to hinder the actuation. An infrared heater was used to ensure any movement of the fabric resulted solely from the mechanical deformation of yarns. The detailed setup can be found in Figure S8 (Supporting Information). Since fabrics tend to relax when removed from the loom, due to inherent residual stresses from weaving, three cycles of heating and cooling were performed with all fabrics. These repetitions allow observing if fabrics can contract and relax to the same positions after heating and cooling. The actuation was recorded with a high-resolution camera^[36] and a thermal camera.

Table 1. Densities of filaments in LCE fabrics of different designs, measured in yarns cm^{-1} .

		Plain	Satin	Rib	Twill
Soft	Warp	24.8	24.9	26.2	27.6
	Weft	19.4	38.5	68.6	59.5
Stiff	Warp	25.3	26.9	25.2	25.0
	Weft	21.4	30.7	54.0	37.9

The typical response of one fabric, in this case with the weft rib structure and soft LCE yarns, being heated and cooled can be seen in Figure 3 (see Movies S7,S8, Supporting Information for other fabrics). In the initial stage, the fabric with length $l = l_0$ was heated from a temperature ranging between 20–30 °C. After reaching the temperature of 120 °C, the infrared heater was turned off and its residual radiation was blocked. The displacement strain, $\epsilon = (l - l_0)/l_0$, of fabrics woven with soft and stiff LCE yarns, can be observed in Figure 3b,c, respectively. Note, the time dependence of this effect is discussed in Figures S13 and S14 (Supporting Information). An evident effect in fabrics using soft LCE yarns with satin, rib, and twill weaving structures is the fact that fabrics are not relaxing to the initial position when cooling. A hysteresis behavior is also observed, and the contraction of the fabrics has reached a plateau at the end of the tested temperature (close to 120 °C). In contrast, for fabrics using stiff LCE yarns, there is little difference in low-temperature positions between the first and the consequent heating cycles, and, therefore, the actuation is fully reversible during the cycles. The recovery of fabrics to their original configurations can be linked with the different elasticity of soft and stiff LCE. Soft LCE fabrics are likely to have residual stresses in

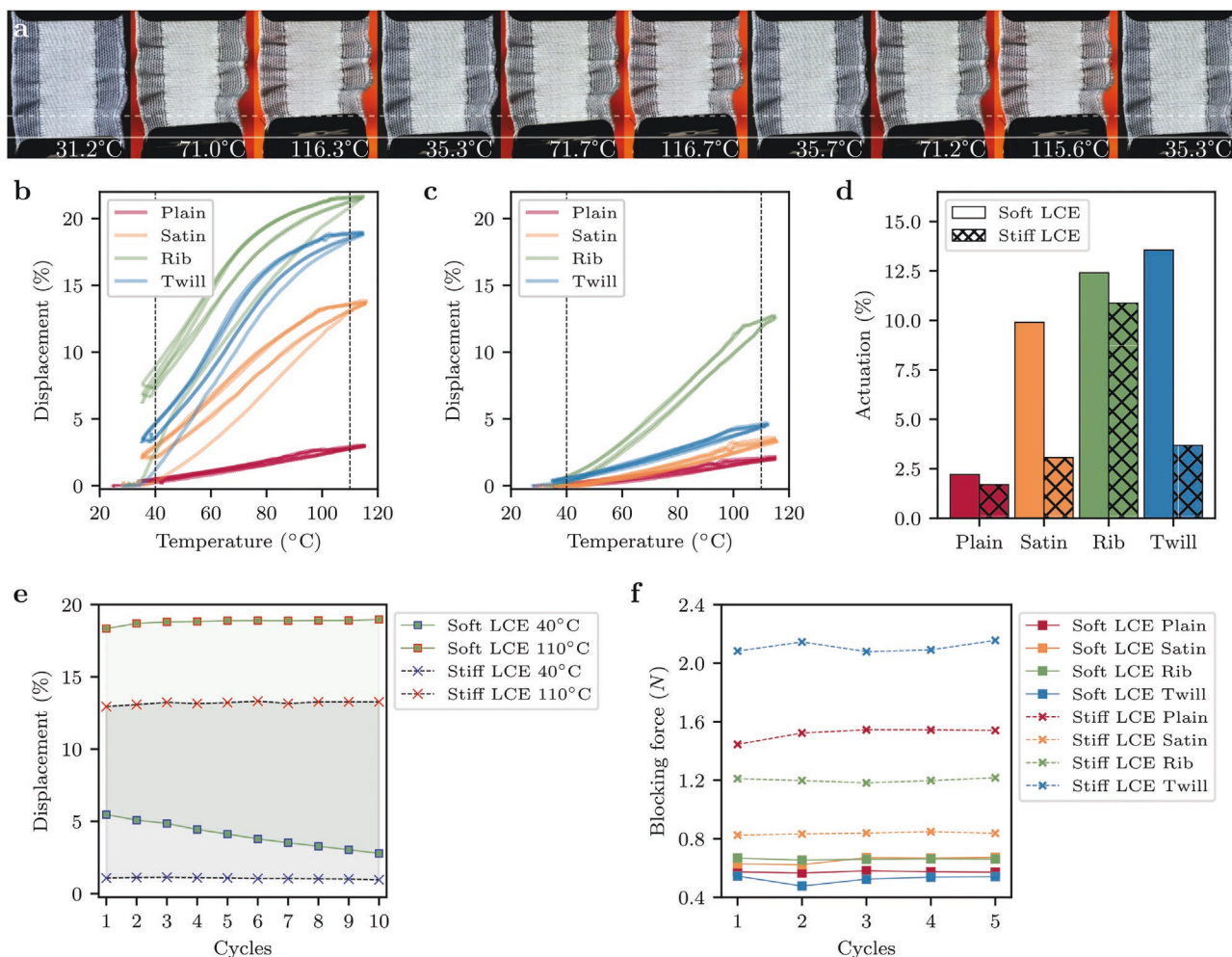


Figure 3. Heating of fabrics with LCE yarn. a) Image sequence of rib fabric using soft yarn heated and cooled three times; full and dashed lines indicate the initial length l_0 and the maximum observed contraction, respectively. b,c) Relative displacement in the function of the temperature for fabrics using soft and stiff yarns; dashed lines indicate the values considered for the performance of actuation. d) Comparison of performances for different weaving constructions and types of yarns; e) Evolution of displacement for ten cycles of heating and cooling of rib fabrics using soft and stiff yarns. No significant attenuation is observed, and the fabric with soft LCE yarns has increased relaxation when compared with the first cycle. f) Blocking force over five cycles. Fabrics using stiff LCE yarns have better performance than fabrics using soft LCE yarns.

fabrics, for instance, when being manipulated to be fixed with metallic clips, and were elongated before the first heating cycle. In addition, the contraction of fabrics using stiff LCE yarns did not reach a plateau in the range of tested temperatures, as expected from the behavior of the single yarn that can be seen in Figure 1.

The overall actuation of the different types of yarns and weaving structures was compared based on the averaged difference of displacements between fabrics reaching 110 °C, when heated, and 40 °C when cooled, Figure 3d. As expected, the actuation increased with the number of floatings. For the range of temperatures used in this work, fabrics with soft LCE performed better than fabrics using stiff LCE. Notably, the rib fabric with stiff LCE has a striking performance, actuating more than two times when compared with the twill fabric with stiff LCE or a similar performance when compared with the rib fabric with soft LCE. By closely looking at the twill fabric with stiff LCE, Figure S18c (Supporting Information),

it is possible to see warp yarns being squeezed into bundles, creating some gaps in floating crossings. Then, despite the warp density being similar in all fabrics, the bundling of the warp yarns gives additional freedom for the weft rib structure to actuate.

Weft rib fabrics using both LCE yarns displayed actuation over 10%. A key characteristic of actuating materials is the stability of the reversible effect, that is, over how many cycles they can maintain the performance, and also the material fatigue. Therefore, we carried out another ten cycles of heating and cooling to check if there was any drift in the actuation for the weft rib fabrics, using soft and stiff LCE yarns. Figure 3e shows that there is no attenuation in the lower and upper limits of the actuation cycle. Similarly, as observed in Figure 3b, upon cooling, the weft rib fabric using soft LCE yarn does not relax to the original position. However, with the increasing number of cycles, this fabric tended to relax closer to its height when starting the experiment.

Apart from the actuation in essentially load-free conditions, the “blocking force” effect under isomeric conditions could also be an important consideration in applications of LCE fabrics. For example, in the medical field, one may require a certain amount of tension to be generated upon LCE actuation, but without significant displacement.^[37] Blocking force refers to the actuation force measured when the length of LCE is fixed. In our case, soft and stiff LCE fabrics with four different weave patterns (same density) were individually clamped in a load cell with a fixed pre-stretch of 10% and their actuation tension force was recorded for five consecutive times. We noticed that while the passive tension (generated by the pre-stretch) was continuously decreasing upon every actuation cycle, possibly through rearrangement of neighboring yarns, Figure S3 (Supporting Information), the amplitude of the tension differences between low and high temperatures (blocking force) remains constant for each fabric sample. Moreover, in line with other tests, the soft/stiff contrast and weave pattern do produce various blocking forces, Figure 3f. All fabrics using soft LCE yarns can generate ≈ 0.6 N of force, with no significant variation between the weaving patterns. A much large disparity was found between fabrics using stiff LCE yarns: the twill fabric produced 2.1 N of blocking force, while the satin fabric could only reach 0.8 N of force. While additional testing is necessary to establish a clear relation between weaving patterns and blocking forces, our results indicate a better performance of the stiff LCE yarn under isomeric conditions.

2.4. A Textile Actuator: from a 2D disc to a 3D Cone

Two well-known problems associated with standard 2D woven fabrics are the rigidity of the woven structure, when compared for instance with knits, and the formation of complex shapes requiring costly and laborious manufacturing.^[38] Here we examine some early steps of integrating the LCE fabric into such designs.

Figure 4 shows an example of developing a 3D fabric design with integrated actuating LCE yarn. Here we combine rigid yarns (linen and nylon) and stiff LCE yarn in a radial-circular weave pattern, aiming to achieve significant 3D shape changes in actuation. The “cone” actuation of a circular LCE director pattern has been theoretically predicted and demonstrated in LCE thin films,^[5,39,40] and here we exploit this topology of deformation while leaving the rigid yarn loops on the outside of the circle for easy sewing into the overall design. The reversible actuation of lifting a cone on heating, and flattening back on cooling is demonstrated in Figure 4d. As with the film-LCE case, there is a significant upward force generated by such a cone. In addition, operating in the textile environment (as opposed to films) allows the combination of yarns of different materials into one functional structure, taking into account typical requirements for smart textiles, such as breathability and user comfort. Taking into account the robustness of the double-network structures in the stiff LCE yarns, we assume their endurance to extend toward washability, which is the topic of further study.

“Smart” wearable fabrics, capable of large reversible actuation, have immediate applications in areas such as sports,

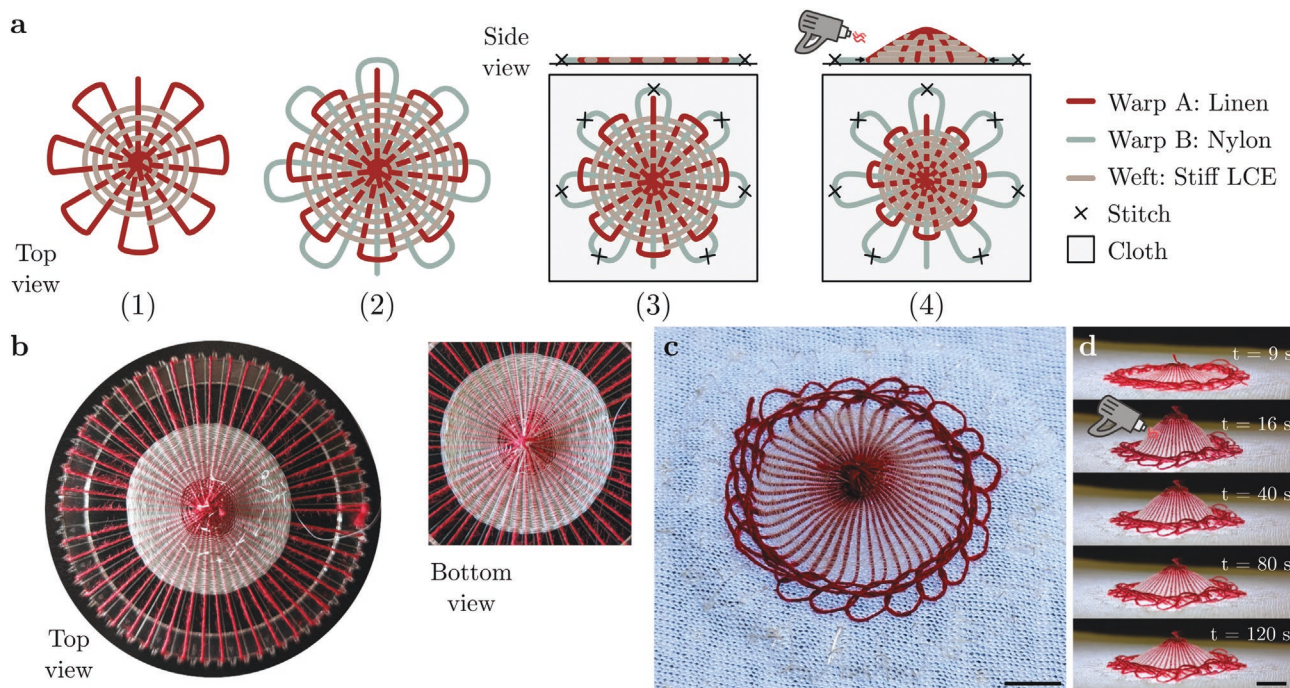


Figure 4. 3D fabric with integrated actuating LCE yarn. a) Illustrations of the steps to build and integrate a disklike smart fabric capable of radial contraction and pop into a cone shape: 1) warp A (linen) yarn is set radially in a circular loom, and LCE yarn is woven in the tangential direction; 2) before finishing the last weaving turns, the warp B (Nylon) is added and the LCE yarn interlaces both warps; 3) next, the fabric is removed from the loom and warp B is stitched to another piece of fabric; 4) upon activation, in this case with a heat gun, the fabric contracts and adopts a conical shape. b) Disc-like fabric at the end of step (2). c) Disc-like fabric after stitching warp B to a knit. d) The integrated fabric is heated between $t = 9$ s and $t = 16$ s with a heat gun; upon heating, the fabric contracts and protrudes into a conical shape; with cooling, the cone-shaped fabric decreases its angle (see Movie S10, Supporting Information). b–d) Scale bar: 1 cm.

rehabilitation, assistive devices, human-computer interfaces, and biomedical technology—and also non-wearable applications exist in, for example, filters, agriculture, thermal insulation, interior design, and room acoustics. In all cases, the tension generated by moderate heating could be translated into the desired effect. It is expected that the LCE phase transition (and consequently the actuation) temperature can be tuned across a wide range—from below ambient to above 120 °C, thus widening the application opportunities. Another prospect often discussed in the literature is to make LCEs actuate by light instead of heating—although the feasibility of how to illuminate significant areas of fabrics with sufficient irradiance without adding bulky light sources is somewhat questionable.

The speed of actuation is mainly regulated by fixed filament properties and weaving constraints, so in the current proof-of-concept work, we did not find any way to significantly increase it. One could, of course, speculate that if the heat could be delivered “faster”, a faster response would be anticipated. However, this would require changing the heating method and involving otherwise unwelcome bulky elements in the fabrics.

Using thin LCE filaments is the key to high response speed. The reason for enclosing such filaments into woven structures is to limit their freedom of random motion and maintain one rigid, elastic entity. However, this limits the range of possible actuation amplitude. We believe that switching from woven structures to, for instance, knits or laces could increase the actuation stroke, but will also change the qualities and consequently the applications of the fabrics themselves.

3. Conclusion

This work brings the exciting ideas of “smart fabrics” one step closer to realization by presenting a proof-of-concept of the integration of LCE yarns with traditional yarns used in the textile industry. Further development of this technology may diversify fashion and e-textile industries, and will eventually contribute to a paradigm shift toward adapting dynamic active textiles. It can also have a transformative effect beyond these obvious domains, for instance, on technical textiles used in agriculture, thermal insulation, interior design, and room acoustics.

Overall, this work showcases both the versatility of liquid crystalline elastomers in fiber form, as well as different textile architectures in creating active responsive fabrics. Even when operating only with a matrix of two different LCE yarns and four commonly-employed weaving patterns, a wide variety of phenomena can be demonstrated. We expect these results to generalize over multiple different triggering stimuli, as well as to other textile crafting techniques in addition to weaving, triggering the rapid development of actuating textiles.

4. Experimental Section

An extended method section of this study is available in the Supporting Information.

The Spinning of LCE Yarn: The extrusion of continuous LCE yarn was performed using a stainless steel syringe mounted on a 3D printer (Engine HR, Hyrel 3D), at a fixed flow rate of 4 $\mu\text{L min}^{-1}$. The

photocuring of the oligomer was achieved along the collection by using three UV-LEDs, with a wavelength of 365 nm and 3 mW cm^{-2} , close to the collection of the filament. Magnesium stearate powder was used to reduce the adhesion properties of the LCE. A cylindrical collector with a diameter of 30 mm rotated at a constant speed of 5 rpm to induce an alignment in the yarn structure. To induce further cross-linking of the LCE material, yarns were submerged into a solution of toluene, at 60 °C for 10 min. Afterward, the swollen yarns were rinsed in acetone and dried in a vacuum oven, at 80 °C for 10 min. Finally, the LCE yarn was exposed to UV light, with a wavelength of 365 nm, for 2 min.

The Weaving of Fabrics using LCE Yarn: The weaves presented in the article were woven by using an AVL Little Weaver table loom, from AVL Looms. The loom had 24 shafts and four heddles were used from every shaft to craft the plain, satin, weft rib and twill weave. The warp was set with a width of 5 cm and the weft was beat up to match the warp yarn density. Additionally, LCE yarns were tested in a custom-built frame loom, and in a Jacquard digital loom (see Section S3.1, Supporting Information). The disk-like fabric capable of actuating into a cone shape was woven in a custom-built circular frame loom.

Heating Testing: A Ryobi hot air blower gun, model EHG2020LCD, was used for localized and fast heating. The heat gun was set in the lowest airflow mode and with a switch-off temperature of 100 °C in the experiments with fabrics. The infrared heating source was a custom-built system composed of 28 quartz heating elements, wavelength of 1.5–8 μm , total wattage of 600 watts, and radiating area of 25 by 25 cm. Metallic clips used in the experiments involving the infrared heater weighed 8.55 g.

Fabrics Measurements: Relative fabrics heights in recordings were measured using a python algorithm, available in the Supporting Information. First, each frame was converted from RGB space into gray space. Next, thresholding was applied to the gray image, where the threshold value was equal to 90 for all recordings. To remove small regions of white or dark spots, three mathematical morphology operations: a dilation, with 20 iterations; an erosion, with 40 iterations; and a second dilation, with 20 iterations were applied to the thresholded image. Finally, a linear fit was applied to each edge between the metallic clips and the fabrics.

Supporting Information

Supporting Information is available from the Wiley Online Library or from the author.

Acknowledgements

This work was supported by the European Research Council (H2020) AdG “Active Polymers for Renewable Functional Actuators” No. 786659, and the European Research Council (H2020) StG “Autonomously adapting and communicating modular textiles” No. 949648. M.V., P.E.S.S., M.M., and J.V. acknowledge the support of the Beyond e-Textiles network, and the Workshops at the School of Chemical Engineering for building a custom-made frame loom. P.E.S.S. acknowledges Emmi Pouta for technical discussions on weaving with a Jacquard loom.

Conflict of Interest

The authors declare no conflict of interest.

Data Availability Statement

The data that support the findings of this study are available on request from the corresponding author. The data are not publicly available due to privacy or ethical restrictions.

Keywords

elastic yarns, elastomers, liquid crystals, smart textiles, soft matter, weaving

Received: November 17, 2022

Revised: January 9, 2023

Published online: February 25, 2023

- [1] M. Warner, E. M. Terentjev, *Liquid crystal elastomers*, Oxford University Press, Oxford, UK **2007**.
- [2] J. Sun, Y. Wang, W. Liao, Z. Yang, *Small* **2021**, *17*, 2103700.
- [3] D. Sun, J. Zhang, H. Li, Z. Shi, Q. Meng, S. Liu, J. Chen, X. Liu, *Polymers* **2021**, *13*, 1889.
- [4] D. Martella, C. Parmeggiani, *Chemistry* **2018**, *24*, 12206.
- [5] T. H. Ware, M. E. Mcconney, J. J. Wie, V. P. Tondiglia, T. J. White, *Science* **2015**, *347*, 982.
- [6] A. Kotikian, C. McMahan, E. C. Davidson, J. M. Muhammad, R. D. Weeks, C. Daraio, J. A. Lewis, *Sci. Rob.* **2019**, *4*, aax7044.
- [7] J. Naciri, A. Srinivasan, H. Jeon, N. Nikolov, P. Keller, B. R. Ratna, *Macromolecules* **2003**, *36*, 8499.
- [8] S. V. Ahir, A. R. Tajbakhsh, E. M. Terentjev, *Adv. Funct. Mater.* **2006**, *16*, 556.
- [9] C. M. Yakacki, M. Saed, D. P. Nair, T. Gong, S. M. Reed, C. N. Bowman, *RSC Adv.* **2015**, *5*, 18997.
- [10] A. Sharma, J. Lagerwall, *Materials* **2018**, *11*, 393.
- [11] X. Lin, M. O. Saed, E. M. Terentjev, *Soft Matter* **2021**, *17*, 5436.
- [12] D. J. Roach, C. Yuan, X. Kuang, V. C.-F. Li, P. Blake, M. L. Romero, I. Hammel, K. Yu, H. J. Qi, *ACS Appl. Mater. Interfaces* **2019**, *11*, 19514.
- [13] Y. Geng, R. Kizhakidathazhath, J. P. F. Lagerwall, *Nat. Mater.* **2022**, *21*, 1441.
- [14] Y. Wang, W. Liao, J. Sun, R. Nandi, Z. Yang, *Adv. Mater. Technol.* **2022**, *7*, 2100934.
- [15] Y. Cheng, R. Wang, K. H. Chan, X. Lu, J. Sun, G. W. Ho, *ACS Nano* **2018**, *12*, 3898.
- [16] Z. Hu, Y. Li, T. Zhao, J.-A. n Lv, *Appl. Mater. Today* **2022**, *27*, 101449.
- [17] C. Wang, X. Jiang, P. Cui, M. Sheng, X. Gong, L. Zhang, S. Fu, *ACS Appl. Mater. Interfaces* **2021**, *13*, 12313.
- [18] Q. He, Z. Wang, Y. Wang, Z. Wang, C. Li, R. Annapooranan, J. Zeng, R. Chen, S. Cai, *Sci. Rob.* **2021**, *6*, abi9704.
- [19] X. Pang, L. Qin, B. o Xu, Q. Liu, Y. Yu, *Adv. Funct. Mater.* **2002451**, **2020**, 30.
- [20] X. Lin, W. Zou, E. M. Terentjev, *Macromolecules* **2022**, *55*, 810.
- [21] *Designing Apparel for Consumers: The Impact of Body Shape and Size*, 1st ed., (Eds.: M.-E. Faust, S. Carrier), Woodhead Publishing, Oxford, UK **2014**.
- [22] X. Nie, S. Wu, P. Lv, H. Ke, F. Huang, Q. Wei, *Chem. Eng. J.* **2022**, *433*, 134410.
- [23] R. Liu, X. Guo, Q. Peng, L. e Zhang, T. T. Lao, T. Little, J. Liu, E. Chan, *Text. Res. J.* **2018**, *88*, 2055.
- [24] H. K. Song, S. P. Ashdown, *Clothing Text. Res. J.* **2012**, *30*, 315.
- [25] Z. Zhou, S. Padgett, Z. Cai, G. Conta, Y. Wu, Q. He, S. Zhang, C. Sun, J. Liu, E. Fan, K. Meng, Z. Lin, C. Uy, J. Yang, J. Chen, *Biosens. Bioelectron.* **2020**, *155*, 112064.
- [26] A. Libanori, G. Chen, X. Zhao, Y. Zhou, J. Chen, *Nat. Electron.* **2022**, *5*, 142.
- [27] J. Stanley, J. A. Hunt, P. Kunovski, Y. Wei, *Eng. Rep.* **2022**, *4*, e12475.
- [28] B. Ridley, J. Chang, L. Bryson, (Other Lab, LLC) US20190269188, **2019**.
- [29] B. Ridley, J. Chang, S. Maikranz, (Other Lab, LLC), US20200399795, **2020**.
- [30] D. R. Merkel, N. A. Traugutt, R. Visvanathan, C. M. Yakacki, C. P. Frick, *Soft Matter* **2018**, *14*, 6024.
- [31] H.-F. Lu, M. Wang, X.-u.-M. Chen, B.-P. Lin, H. Yang, *J. Am. Chem. Soc.* **2019**, *141*, 14364.
- [32] T. Ohzono, Y. Norikane, M. O. Saed, E. M. Terentjev, *ACS Appl. Mater. Interfaces* **2020**, *12*, 31992.
- [33] H. J. Farre-Kaga, M. O. Saed, E. M. Terentjev, *Adv. Funct. Mater.* **2022**, *32*, 2110190.
- [34] S. Adanur, *Wellington Sears handbook of industrial textiles*, Technomic Pub, Lancaster, PA, USA **1995**.
- [35] A. Albers, N. F. Weber, M. Cirauqui, T. L. Smith, *On weaving*, Princeton University Press, Princeton, NJ, USA **2017**.
- [36] K. Miikki, A. Karakoç, M. Rafiee, D. W. Lee, J. Vapaavuori, J. Tersteegen, L. Lemetti, J. Paltakari, *SoftwareX* **2021**, *14*, 100688.
- [37] C. Ferrantini, J. M. Pioner, D. Martella, R. Coppini, N. Piroddi, P. Paoli, M. Calamai, F. S. Pavone, D. S. Wiersma, C. Tesi, E. Cerbai, C. Poggesi, L. Sacconi, C. Parmeggiani, *Circ. Res.* **2019**, *124*, e44.
- [38] J. Underwood, *PhD Thesis*, RMIT University, Melbourne, Australia **2009**.
- [39] C. D. Modes, K. Bhattacharya, M. Warner, *Proc. Math. Phys. Eng. Sci.* **2011**, *467*, 1121.
- [40] B. A. Kowalski, C. Mostajeran, N. P. Godman, M. Warner, T. J. White, *Phys. Rev. E* **2018**, *97*, 012504.